XIV International Conference on Computational Plasticity. Fundamentals and Applications
COMPLAS 2017
E. Oñate, D.R.J. Owen, D. Peric and M. Chiumenti (Eds)

ANALYSIS OF PRE-TENSIONED STRUCTURES BY MEANS OF A CONSTITUTIVE SERIAL-PARALLEL RULE OF MIXTURES

L. G. BARBU[*], C. ESCUDERO[†], A. CORNEJO[†], X. MARTINEZ[†], S. OLLER[†] AND A. H. BARBAT[†]

[*, †]International Center for Numerical Methods in Engineering (CIMNE)
Universidad Politécnica de Cataluña
Campus Norte UPC, 08034 Barcelona, Spain
e-mail: lgratiela@cimne.upc.edu

Key words: Pre-stressed concrete, Rule of mixtures, Composites, FEM.

Abstract. The main purpose of this paper is to develop a reliable method based on a three-dimensional (3D) finite-element (FE) model to simulate the constitutive behaviour of reinforced concrete structures strengthened with post-tensioned tendons. A 3D FE model was used, where the nonlinear material behaviour and geometrical analysis based on incremental–iterative load methods were adopted. The pre-tensioned concrete is modelled as a composite material whose behaviour is described with the serial-parallel rule of mixtures (S/P RoM) [1-3]. The effective pre-tensioning stress was applied as an initial strain imposition in the steel material used to model the tendons. The methodology is valid for both straight and curvilinear steel tendons. Examples of both cases will be shown. Validation by comparison with the analytic solution is done for the case of a concrete beam with a straight pre-tensioned steel tendon embedded. Other examples are also included.

1 INTRODUCTION AND STATE OF THE ART

Pre-stressing a structure consists in introducing a system of forces previously to the action of the external loads, with the objective of achieving an equilibrium state without tensions or cracking. In order to carry out a pre-stressing system it is mandatory to use some high performance materials in terms of the concrete and the steel used in the pre-stressing tendons. One of the main advantages of the pre-stressing system is the reduction of the material needed in order to build a certain structure due to the increase of the efficiency of the concrete, whose behaviour is better in compression. The already mentioned pre-compression of the concrete induced by the steel tendons can reduce or even remove the cracks at short and long term, enhancing the durability and impermeability of the material.

One of the most commonly used methods to simulate the pre-stressed system (for straight and parabolic shaped tendons) consists in adding concentrated loads at the anchoring zones and an ascending distributed load that represents the effect of the curvature of the tendon along its path [4]. The mentioned method is simple and straightforward but is limited to simple geometries in which the equivalent uniform effect of the pre-stressing can be computed analytically. A more sophisticated method consists in simulating the continuum by means of

finite elements (tetrahedral and hexahedral in general) and artificially add biarticulated elements connecting pairs of nodes that create the effect of the post tensioned tendons [5]. The previous method achieves satisfactory results but, implicitly, the mesh is conditioned by the path of the tendons whose trajectory has to connect nodes of the finite element mesh. This conditioning can be challenging when meshing. In addition, the sliding between the steel tendon and the concrete cannot be added as occurs in real cases.

The formulation shown in this article requires only a finite element mesh of any type and any spatial discretization. In this case the steel tendons are taken into account in a constitutive way, which means that the active steel is a component of the composite material of each finite element of the mesh that coincides with (is intersected by) the path of the tendon. This implies that the stress and strain state at each integration point is computed from the participation of each component inside the influence zone of that integration point. This global participation results of imposing the equilibrium and/or compatibility between the simple materials at each point, by means of a formulation called Serial-Parallel Rule of Mixtures. Applying the mentioned theory one can assume that each material behaves following its own constitutive law (elasticity, damage, plasticity, viscoelasticity, etc.). The same formulation takes into account all the materials in order to obtain the behaviour of the composite. Finally, the pre-stressing is introduced as an initial imposed strain in the active steel which is going to be partially compensated by the concrete. Next, the displacement field is updated until a global convergence of forces is achieved.

2 CONSTITUTIVE MODELLING OF PRE-STRESSED REINFORCED CONCRETE WITH THE SERIAL-PARALLEL RULE OF MIXTURES

The serial/parallel mixing theory (S/P RoM) is based on the definition of two different compatibility equations between the strain and stress states of the composite constituent materials: it defines an iso-strain condition on the parallel direction, usually the fiber direction, and it defines an iso-stress condition on the serial direction, usually the remaining directions. Using these compatibility equations in a composite made of matrix and fiber, if the matrix structural capacity is lost due to excessive shear stresses, the iso-stress condition also reduces the shear capacity of fiber, and consequently the composite serial strength is also reduced.

For this reason, it is necessary to define, and split, the serial and parallel parts of the strain and stress tensors. This is done with two complementary fourth order projector tensors, one corresponding to the serial direction (P_S) and the other to the parallel direction (P_P). These tensors are defined from the fibre axial direction in the composite. Thus,

$$\varepsilon = \varepsilon_P + \varepsilon_S \quad \text{with} \quad \varepsilon_P = P_P : \varepsilon \quad \text{and} \quad \varepsilon_S = P_S : \varepsilon \tag{1}$$

where,

$$P_S = I - P_P ; \; P_P = N_P \otimes N_P \text{ and } N_P = e_1 \otimes e_1 \tag{2}$$

Being e_1 , the director vector that determines the parallel behaviour (fibre direction), and I the identity. The stress state may be split analogously, finding its parallel and serial parts using also the 4th order tensors P_P and P_S :

$$\sigma = \sigma_P + \sigma_S \text{ with } \sigma_P = P_P : \sigma \text{ and } \sigma_S = P_S : \sigma \tag{3}$$

3.1 Hypothesis for the numerical modelling

The numerical model developed to take into account this strain-stress state is based on the following hypothesis:

1. The composite is composed by only two components: fibre and matrix
2. Component materials have the same strain in parallel (fibre) direction.
3. Component materials have the same stress in serial direction.
4. Composite material response is in direct relation with the volume fractions of compounding materials.
5. Homogeneous distribution of phases is considered in the composite.
6. Perfect bounding between components is also considered.

3.2 Constitutive equations of component materials

Each composite component material is computed with its own constitutive equation. However, as in this paper the materials will be modelled with a damage formulation, the description of the formulation is done considering the particular case of isotropic damage. So, the stresses in matrix and fibre materials are obtained using:

$$\begin{aligned} {}^{m}\sigma &= (1-{}^{m}d)\cdot {}^{m}C : {}^{m}\varepsilon \\ {}^{f}\sigma &= (1-{}^{f}d)\cdot {}^{f}C : {}^{f}\varepsilon \end{aligned} \tag{4}$$

being ${}^{m}C$ and ${}^{f}C$ the matrix and fibre stiffness tensors, respectively. These equations can be rewritten taking into account the serial and parallel split of strain and stress tensors (equations (1) and (3)), obtaining:

$$\begin{bmatrix} {}^{i}\sigma_P \\ {}^{i}\sigma_S \end{bmatrix} = (1-{}^{i}d)\cdot \begin{bmatrix} {}^{i}C_{PP} & {}^{i}C_{PS} \\ {}^{i}C_{SP} & {}^{i}C_{SS} \end{bmatrix} : \begin{bmatrix} {}^{i}\varepsilon_P \\ {}^{i}\varepsilon_S \end{bmatrix} \tag{5}$$

where

$$\begin{aligned} {}^{i}C_{PP} &= P_P : {}^{i}C : P_P & {}^{i}C_{PS} &= P_P : {}^{i}C : P_S \\ {}^{i}C_{SP} &= P_S : {}^{i}C : P_P & {}^{i}C_{SS} &= P_S : {}^{i}C : P_S \end{aligned} \quad \text{with } i = m, f \tag{6}$$

3.3 Equilibrium and compatibility equations

The equations that define the stress equilibrium and establish the stain compatibility between components arise from the analysis of the hypotheses previously exposed,

Parallel behaviour:
$$\begin{aligned} {}^{c}\varepsilon_P &= {}^{f}\varepsilon_P = {}^{m}\varepsilon_P \\ {}^{c}\sigma_P &= {}^{f}k \cdot {}^{f}\sigma_P + {}^{m}k \cdot {}^{m}\sigma_P \end{aligned} \tag{7}$$

Serial behaviour:
$$\begin{aligned} {}^{c}\varepsilon_S &= {}^{f}k \cdot {}^{f}\varepsilon_S + {}^{m}k \cdot {}^{m}\varepsilon_S \\ {}^{c}\sigma_S &= {}^{f}\sigma_S = {}^{m}\sigma_S \end{aligned} \tag{8}$$

where superscripts c , m and f stand for composite, matrix and fibre, respectively and ${}^{i}k$ corresponds to the volume fraction coefficient of each constituent in the composite.

3.4 Serial/parallel rule of mixtures algorithm

The known variable that enters the algorithm is the strain state ${}^{c}\varepsilon$ of the composite material at time $t+\Delta t$. From this variable, the serial/parallel rule of mixtures algorithm has to find the strain and stress state of each component that fulfils the equilibrium, the compatibility and the constitutive equations and the evolution of the internal variables. The first thing done by the algorithm is to split the strain tensor into its parallel and its serial parts, in order to compute the strain state in the matrix and the fiber. The parallel strain component is, according to equation (7), the same for both materials and for the composite. On the other hand, the serial strain component requires a prediction of the strains expected in one of the composite components. If this prediction is done for the matrix, the increment of its serial strains can be computed as

$$\left[{}^{m}\Delta\varepsilon_S\right]^{0} = A : \left[{}^{f}C_{SS} : {}^{c}\Delta\varepsilon_S + {}^{f}k \cdot \left({}^{f}C_{SP} - {}^{m}C_{SP}\right) {}^{c}\Delta\varepsilon_P\right] \tag{9}$$

with $A = \left[{}^{m}k \cdot {}^{f}C_{SS} + {}^{f}k \cdot {}^{m}C_{SS}\right]^{-1}$ and ${}^{m}\Delta\varepsilon_S = {}^{t+\Delta t}\left[{}^{c}\varepsilon_S\right] - {}^{t}\left[{}^{c}\varepsilon_S\right]$.

The initial prediction of matrix serial strains, proposed by Rastellini [1] and described in equation (9), is obtained considering that the distribution of the total strain, in its parallel and serial parts, is done in function of the composite tangent stiffness obtained in previous time step. With the prediction of the matrix serial strains, the fibre serial strains can be computed, in the iteration step *n*, according to equation (8),

$${}^{t+\Delta t}\left[{}^{f}\Delta\varepsilon_S\right]^{n} = \frac{1}{{}^{f}k}\,{}^{t+\Delta t}\left[{}^{c}\varepsilon_S\right] - \frac{{}^{m}k}{{}^{f}k}\,{}^{t+\Delta t}\left[{}^{m}\varepsilon_S\right]^{n} \tag{10}$$

where ${}^{t+\Delta t}\left[{}^{m}\varepsilon_S\right]^{n} = {}^{t}\left[{}^{m}\varepsilon_S\right] + \left[{}^{m}\Delta\varepsilon_S\right]^{n}$.

Regrouping again the serial and parallel components of the strain tensor (equation (3)), the constitutive equations can be applied to the predicted strains to obtain the stress tensor for both materials and the update of their internal variables. Fibre and matrix are modelled, each one, with their own constitutive law. If both materials are described with an additive plasticity formulation, the stress vector for each one is obtained using equation (4). The stresses obtained must fulfil the following equation:

$$[\Delta\sigma_S]^n = {}^{t+\Delta t}[{}^m\sigma_S]^n - {}^{t+\Delta t}[{}^f\sigma_S]^n \leq toler \tag{11}$$

If the residual stress is smaller than the tolerance, the computed strains and stresses are considered to be correct and the structural calculation can continue. However, if equation (11) is not fulfilled, the initial prediction of the matrix strain tensor has to be corrected. This correction is performed using a Newton-Raphson scheme, in which the update is made using the Jacobian of the residual forces. It is obtained deriving the residue function with respect to the unknown. According to Rastellini [1], the expression for the Jacobian is given as follows:

$$J = [{}^mC^t_{SS}]^n + \frac{{}^mk}{{}^fk} \cdot [{}^fC^t_{SS}]^n \tag{12}$$

and, the correction of the matrix serial strains becomes

$${}^{t+\Delta t}[{}^m\varepsilon_S]^{n+1} = {}^{t+\Delta t}[{}^m\varepsilon_S]^n - J^{-1} : [\Delta\sigma_S]^n \tag{13}$$

To obtain quadratic convergence in the S/P mixing theory, the Jacobian must be obtained using the tangent constitutive tensors for the fibres and the matrix. Depending on the constitutive equation defined for each material, the constitutive tensor cannot be obtained analytically. Thus, in order to obtain a reliable algorithm, the expression of the tangent tensor is obtained numerically with the procedure shown in Martinez et al. [1][3].

3.5 Peculiarities of the imposed strain loading

The theoretical frame developed in the previous sections suffices to represent the behaviour of reinforced concrete as a composite material composed by concrete and passive steel. In order to take into account the case of the active steel, both for the pre and the post-tensioned case, it is necessary to rewrite the compatibility condition of the S/P RoM.

Specifically, it is necessary to break the perfect adherence between the two components: active steel and concrete.

6. Relative movement between the components is allowed if and only if an imposed strain condition exists over one of them.

Therefore, loss of adherence is allowed only in the presence of the imposed strain loading, a peculiar load due to the fact that it is applied only on a component of the composite material. This implies that its contribution is not quantified in the external forces vector and it is an auto balanced load.

Equations (7) must therefore be rewritten taking into account the imposition of an initial strain for the fiber in order to represent the pre-stressing or post-tensioning of the active steel. In the first iteration of the increment when the pre-stressing strain is to be applied, the fiber strain in the parallel direction is fixed to the desired pre-stress value. Based on the serial fiber strains (obtained with eq. (10)) and the parallel ones (eq. (14)) the fiber strain tensor is computed and, depending on the desired fiber constitutive model, the stress tensor is obtained.

The resolution algorithm of the S/P RoM equilibrates the serial components at each integration point and with the integrated stresses the internal forces vector is assembled. At this point in the problem resolution, the parallel component of the fiber stresses has yet to be balanced. Its effect is quantified in the system of equations in the residual forces computed at the end of the first global iteration of the problem.

$$\begin{aligned} incr = 1; iter = 1; \quad & {}^{m}\varepsilon_P = {}^{c}\varepsilon_P \\ & {}^{f}\varepsilon_P = \varepsilon_{imp} \\ incr \geq 1; iter > 1; \quad & {}^{m}\varepsilon_P = {}^{c}\varepsilon_P \\ & {}^{f}\varepsilon_P = {}^{c}\varepsilon_P + \varepsilon_{imp} \end{aligned} \tag{14}$$

These residual forces are then used to correct the nodal displacements and consequently the strains at the integration points. In the second global iteration of the problem, the parallel component of the strains at layer level that is the input of the S/P RoM is equal to the matrix strain needed to accommodate the imposed fiber strain.

Therefore, in the first global iteration the active steel has its parallel strain component fixed at the level of strain associated to the desired pre-stressing force, while in the second iteration the fiber strain is balanced by the resulting compression in the concrete.

3 VALIDATION OF THE FORMULATION

In this section some examples of application of the formulation shown in this article are presented. The two fist examples are compared with the expected analytical solution since their geometry is sufficiently simple to be solved. In the third example, a more complex problem has been analysed, so in this case the solution cannot be compared with any analytical expression.

3.1 Pre-stressed beam with a straight tendon

In this example, the behaviour of a 7 m length and 1 m quadrangular beam is analysed. Aligned with the center of gravity of the beam there is a linear steel tendon whose area, A_s, is equal to 0.04 m^2 which means that the participation with respect to the concrete is 4%. The geometry of the specimen can be appreciated in the Fig 1a. The self-weight has been neglected in order to focus on the pre-stressing effect. In addition, one edge of the beam is free and the other one is clamped.

The geometry shown in the Fig. 1a has been meshed with linear hexahedral finite elements obtaining the finite element mesh depicted in the Fig. 1b. The pre-stressed tendon has been stressed up to 1176 Mpa, corresponding to a strain, ε_s, equal to 0.0056. The Young's modulus of the steel has been considered to be 210000 MPa whereas the concrete modulus is equal to 35000 Mpa.

The axial force in the steel tendon can be computed using the equation (15). On the other hand, the elastic shortening of the concrete can be obtained by means of the equation (16). Finally, the longitudinal displacement of the whole beam due to the pre-stressing load can be calculated using the equation (17). The finite elements intersected by the tendon can be seen in

the Fig. 1c. Those elements, which have a certain participation of active steel, will have an imposed strain loading condition, simulating the effect of the pre-stressing.

$$N_t = A_s\,\sigma_t = 4.704 \cdot 10^7\ N \tag{15}$$

$$\Delta\varepsilon = -\frac{N_t}{E_c A_c + E_s A_s} = -1{,}12 \cdot 10^{-3} \tag{16}$$

$$\delta_{long} = \Delta\varepsilon \cdot L = -7{,}840 \cdot 10^{-3}\ m \tag{17}$$

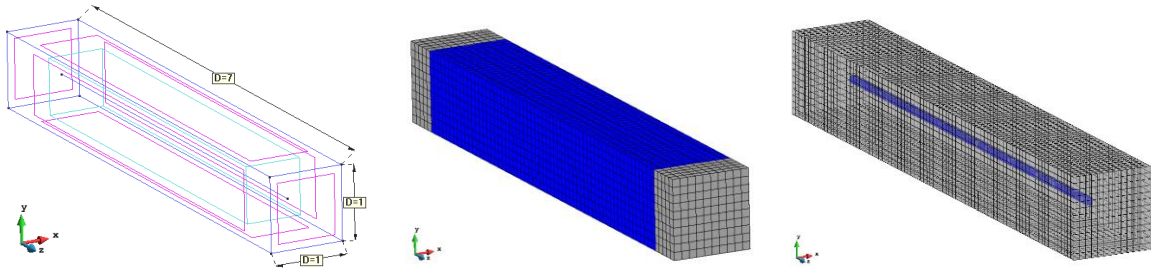

Figure 1. a) Geometry of the beam; b) Finite element mesh (7000 elements); c) Elements intersected by the steel tendon

Carrying out the calculation with the finite element code PLCd [6-9], one can obtain the displacement field shown in the Fig. 2. As can be seen in the previous figure, the maximum shortening of the beam has a value of $7.83 \cdot 10^{-3}$ m whereas the analytical solution is $7.84 \cdot 10^{-3}$ m. This result shows the high precision of the formulation.

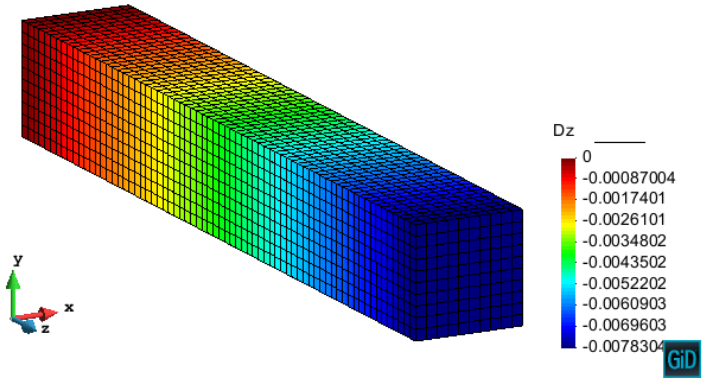

Figure 2. Displacement field as resulting from the pre-stressing

3.2 Pre-stressed beam with a curvilinear tendon

In this case, a 10 m length and 1 m height beam has been simulated. In order to increase the complexity of the pre-stressing system, the steel tendon has a parabolic shaped curve, as is commonly used in pre-stressed beams. The geometry is shown in the Fig 3 and the local axes of the active steel can be seen in the Fig. 4a. Each colour in the Fig. 4b represents a different composite material in terms of steel participation as well as its direction since the slope of the

tendon is not constant. The steel tendon has been pre-stressed with a force, P, equal to 5000 kN and has an area of 0.005 m^2. One can easily notice that the stress in the tendon is 1000 Mpa. The concrete used in the simulation has a Young's modulus, E_c, equal to 35875 Mpa.

The finite element mesh depicted in the Fig. 4a consists of 1288 linear hexahedra. In the same figure one can see the different composite materials existent inside the beam.

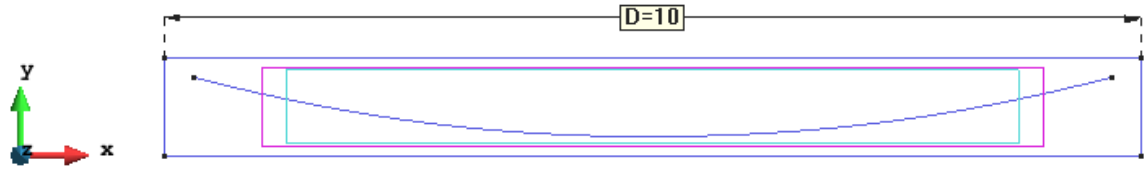

Figure 3. Geometry of the beam and of the steel tendon

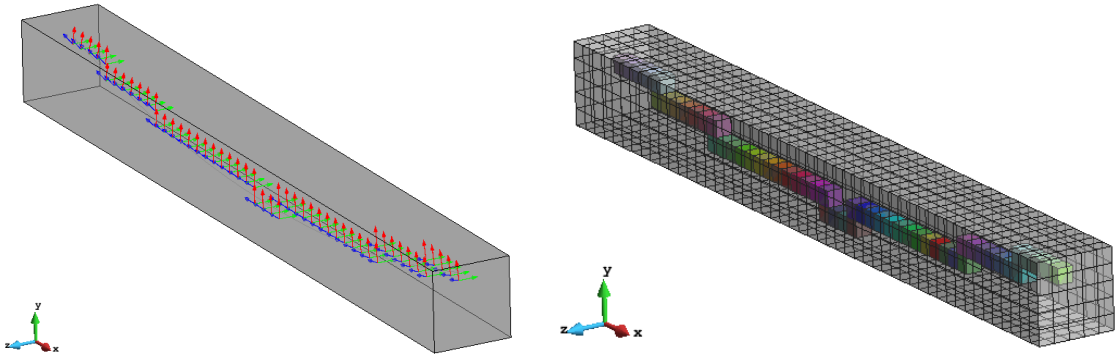

Figure 4. a) Local axes of the tendon on the finite elements; b) Finite element mesh used

In order to compute the analytical vertical displacement, one must simplify the structural system as can be seen in the Figs. 5 and 6. In the Fig. 6 one can appreciate the equivalent load system that simulates the effect of the pre-stressing force. In this case, the steel tendon has been substituted with two concentrated loads in the anchoring zone and, due to the eccentricity in the anchoring zone, two bending moments. The parabolic shape is represented by a uniformly distributed load whose value is obtained with the equation (18).

$$\eta = \frac{8P(e_1 + e_2)}{L^2} = 240\,\frac{kN}{m} \tag{18}$$

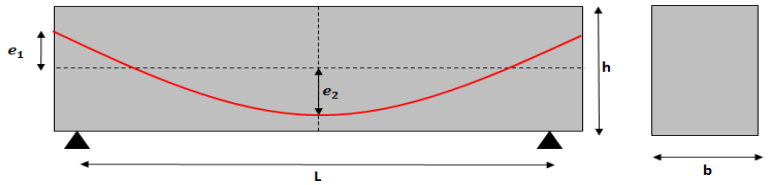

Figure 5. Schematic representation of the beam

By means of tables and the superposition hypothesis, one can obtain the analytical expression of the maximum vertical displacement of the beam (18). It is important to notice that the tables, in general, omit the effect of the shear strain as well as the elastic shortening of the concrete.

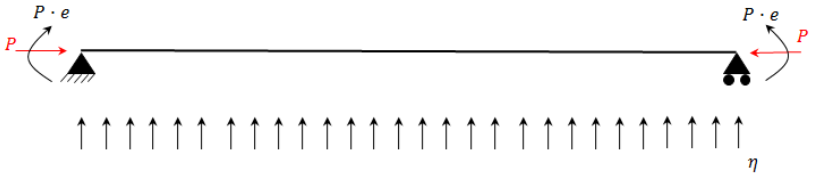

Figure 6. Structural scheme of the beam with one curvilinear tendon

$$\delta = \frac{5\eta L^4}{384 E_h I} - \frac{3P\cos(\phi) e_1 L^2}{24 E_h I} = 4.38 \text{ mm} \tag{19}$$

where E_h corresponds to the Young's modulus of the homogenized section, I is the inertia of the section and ϕ is the slope of the tendon in the anchoring zone.

Using the in-house finite element code PLCd, one can obtain the displacement field depicted in the Fig. 7 with a maximum vertical displacement equal to 4.60 mm. Comparing the expected results with the simulated ones, the difference between them assuming that the analytical is exact, which is not entirely correct, is about a 5%. Additionally, the stress field for each simple material can be seen in the Figs. 8 and 9. As indicated in the previous figures, the pre-stressing system induces a bending state in the structure that causes tension on the superior fibre and compression on the lower fibre which compensates the effect of the self-weight. The stress field of the steel oscillates between the 900-1000 Mpa as has been indicated in the previous paragraphs. The mentioned variation is caused by the elastic shortening of the concrete.

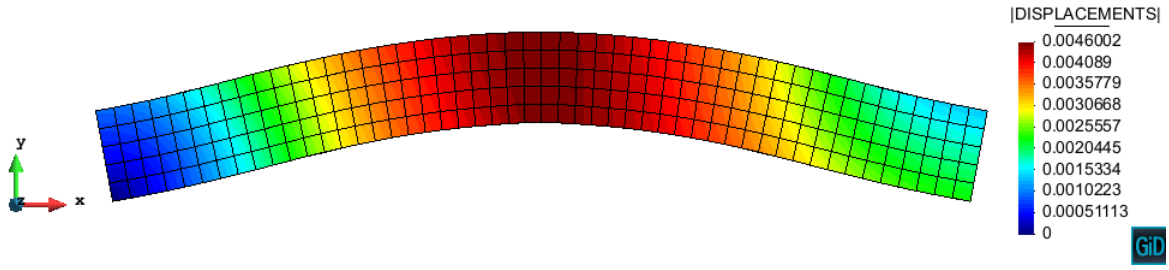

Figure 7. Displacement field obtained with PLCd

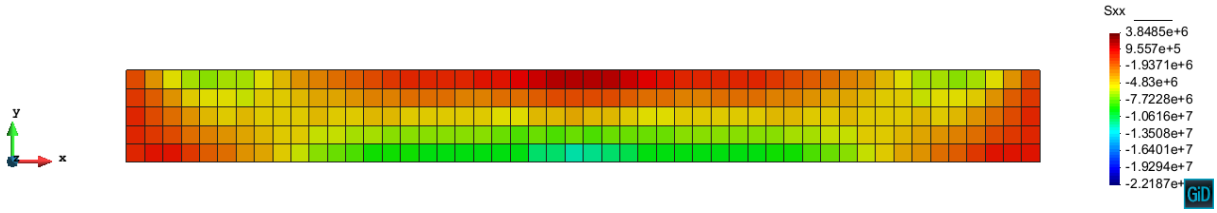

Figure 8. Longitudinal stresses S_{xx} in the concrete

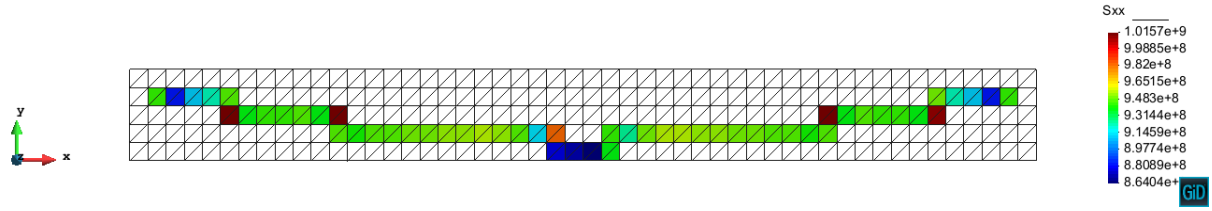

Figure 9. Longitudinal stresses S_{xx} in the active steel

3.3 Concrete ring reinforced with pre-stressed tendons

In order to analyse a more complex geometry, a three-dimensional model of a 10 m height and 1.15 m thickness concrete ring is shown. The structure is stiffened with 3 buttresses (spaced 120º) and reinforced with 3 steel tendons whose anchoring zone coincides with the position of the buttresses. In Fig. 10 the geometry of the analysed structure is depicted, as well as the finite element mesh that consists of 69324 linear hexahedra elements.

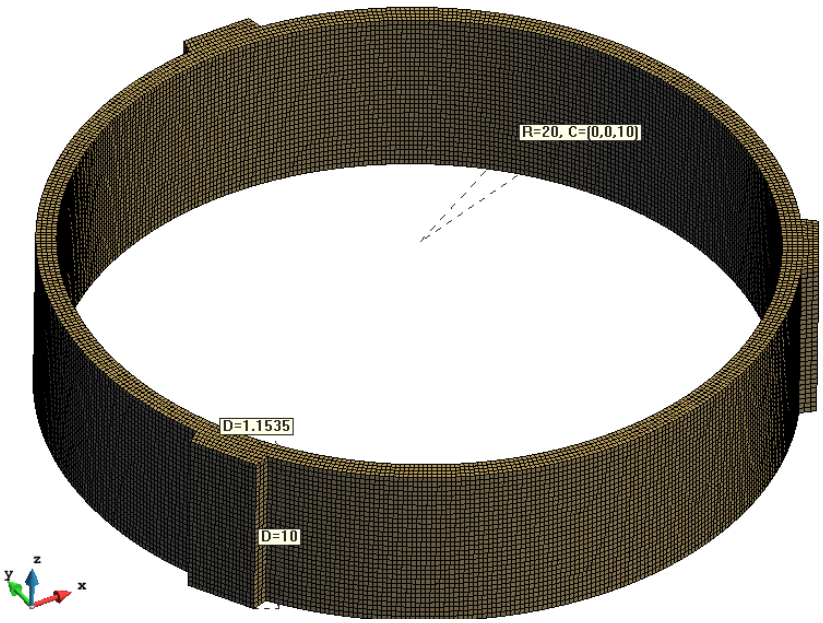

Figure 10. Geometry and finite element mesh of the ring

In Fig. 11a the trajectory of the three steel tendons can be seen. In the same figure one can notice that each tendon covers 240º of the annular section. Those tendons have a diameter of 0.082 m and have been pre-stressed with an imposed strain of 0.0062. The corresponding stress in each tendon is 1302 Mpa.

As explained in previous paragraphs, the finite elements intersected by the linear elements (tendons) have a certain participation of active steel inside the composite material as well as a certain orientation of it. The mentioned orientation (local axes) of the steel can be analysed in the Fig. 11b for each tendon.

The results of the numerical simulation are depicted in the Figs. 12 and 13. As expected, the central part of the ring experiences a deformation inwards. This tendency is smoother near the buttresses where the stiffness is greater, as expected.

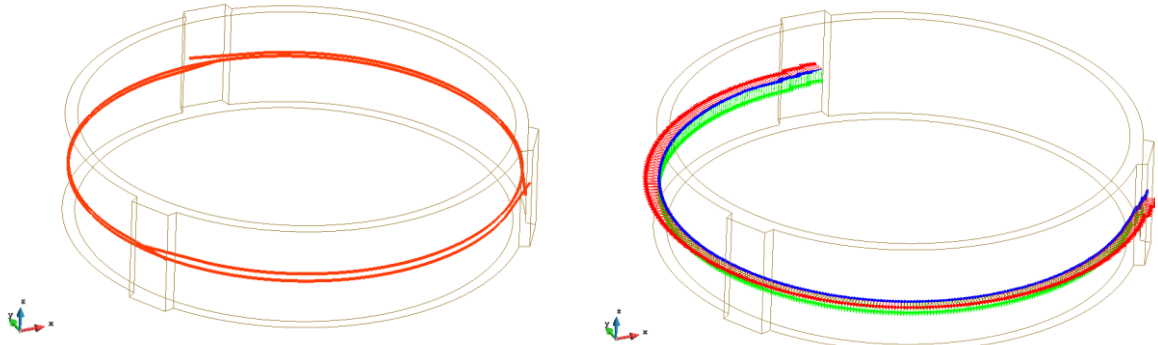

Figure 11. a) Schematic trajectory of the steel tendons; b) Local axes of the finite elements intersected by the tendon

The Figs. 13a and 13b represent a horizontal cut of the ring in the x-y plane showing the stress state in the two composite components, steel and concrete. The mentioned cut coincides with the path of one of the tendons so, in this case, one can appreciate the local effect of that tendon.

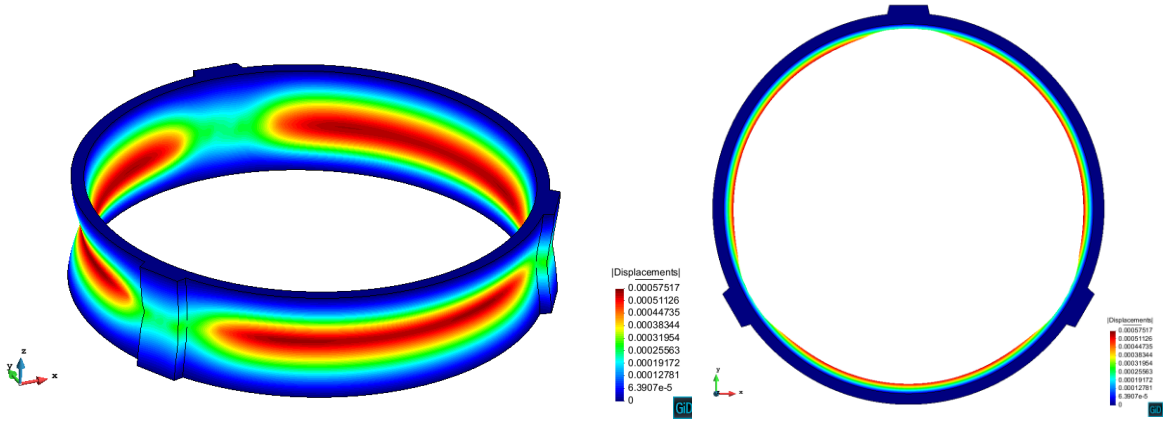

Figure 12. Displacement field in m on the deformed shape of the geometry (100x)

In the Fig. 13a, the concrete is fully compressed except for the anchoring zone where, in general, a large quantity of passive reinforcement is placed to compensate this effect that would lead to the cracking of the concrete.

On the other hand, in Fig. 13b, one can observe that the steel tendon is completely tensioned. It is important to note that the stress along the tendon is not constant, being minimum in the mid-point of it.

4 CONCLUSIONS

As has been shown in the previous paragraphs, the current formulation is capable of simulating the effect of the pre-stressed system in arbitrary geometries and obtains coherent results with a reduced error in comparison with the most used methods to deal with similar problems. That said, one can conclude that the formulation presented in this article represents a powerful tool when dealing with complex geometries or sophisticated constitutive models of composite materials.

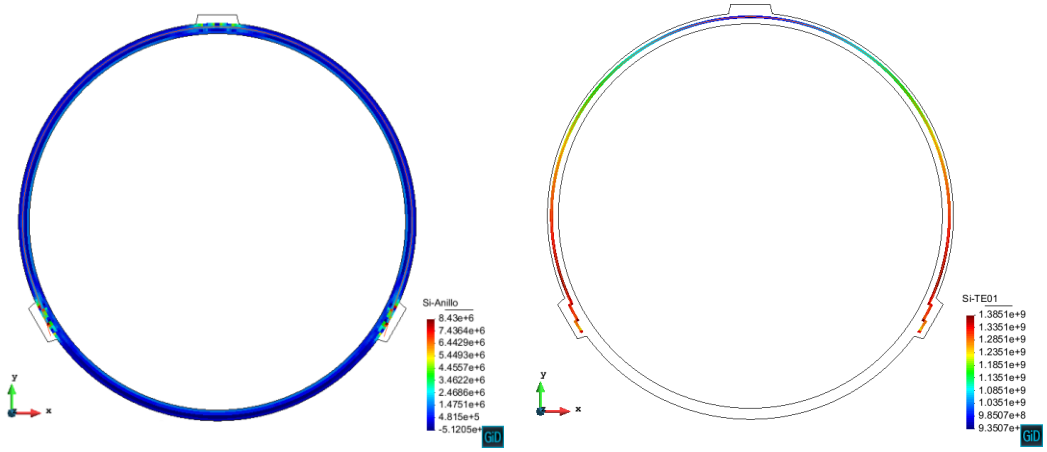

Figure 13. a) Stress field S_1 in the concrete; b) Stress field S_1 in the active steel

REFERENCIAS

[1] Rastellni, F., Oller, S., Salomon, O., Oñate, E.: Composite materials non-linear modelling for long fibre reinforced laminates: Continuum basis, computational aspects and validations. *Computers and Structures* (2008) **86**(9), 879-896.

[2] Martinez, X., Oller, S., Rastellini, F. and Barbat, A. A numerical procedure simulating RC structures reinforced with FRP using the serial/parallel mixing theory, *Computers and Structures*, (2008) **86**(15-16):1604-18.

[3] Martinez, X., Oller, S., Rastellini, F. *Análisis no-lineal de materiales compuestos mediante la teoría de mezclas serie-paralelo*. Omnia Publisher, 2014. Capítulo 10 - p. 237-260. Libro: Aplicaciones avanzadas de los materiales compuestos en la obra civil y la edificación, (http://dx.doi.org/10.3926/oms.209)

[4] Rezaie, F., Famam, S.M. Fracture mechanics analysis of pre-stressed concrete sleepers via investigating crack initiation length. *Engineering Failure Analysis* 58 (2015) 267–280.

[5] Shokoohfar, A., Rahai, A. Nonlinear analysis of pre-stressed concrete containment vessel (PCCV) using the damage plasticity model. *Nuclear Engineering and Design* 298 (2016) 41–50.

[6] PLCd Manual. Non-linear thermo-mechanic finite element code oriented to PhD student education. Code developed at CIMNE; 1991–to present. URL: <http://www.cimne.com/plcd>.

[7] Barbu, L.G., Oller, S., Martinez, X. and Barbat, A. High cycle fatigue simulation: A new stepwise load-advancing strategy, *Engineering Structures* (2015) 97: 118-129, http://dx.doi.org/10.1016/j.engstruct.2015.04.012.

[8] Barbu, L.G., Martinez, X., Oller, S. and Barbat, A.H. Validation on large scale tests of a new hardening-softening law for the Barcelona plastic damage model, *Int. J. Fat*. 2015; 81:213-226.

[9] Martinez, X., Oller, S., Barbu, L., Barbat, A. and De Jesus, A.M.P., 2015. Analysis of ultra-low cycle fatigue problems with the Barcelona plastic damage model and a new isotropic hardening law, *Int. J. Fatigue*, 73, pp 132-142.